



HAL
open science

Implication of a Silyl Cobalt Dihydride Complex as a Useful Catalyst for the Hydrosilylation of Imines

Cassandre C Bories, Marion Barbazanges, Etienne Derat, Marc Petit

► **To cite this version:**

Cassandre C Bories, Marion Barbazanges, Etienne Derat, Marc Petit. Implication of a Silyl Cobalt Dihydride Complex as a Useful Catalyst for the Hydrosilylation of Imines. ACS Catalysis, 2021, pp.14262-14273. 10.1021/acscatal.1c03886 . hal-03425497

HAL Id: hal-03425497

<https://hal.science/hal-03425497>

Submitted on 10 Nov 2021

HAL is a multi-disciplinary open access archive for the deposit and dissemination of scientific research documents, whether they are published or not. The documents may come from teaching and research institutions in France or abroad, or from public or private research centers.

L'archive ouverte pluridisciplinaire **HAL**, est destinée au dépôt et à la diffusion de documents scientifiques de niveau recherche, publiés ou non, émanant des établissements d'enseignement et de recherche français ou étrangers, des laboratoires publics ou privés.

Implication of a Silyl Cobalt Dihydride Complex as a Useful Catalyst for the Hydrosilylation of Imines

*Cassandra C. Bories, Marion Barbazanges, Etienne Derat and Marc Petit**

Sorbonne Université, CNRS, Institut Parisien de Chimie Moléculaire, UMR 8232, 4 place Jussieu, 75005 Paris, France.

Cobalt, imine reduction, hydrosilylation, DFT, homogeneous catalysis

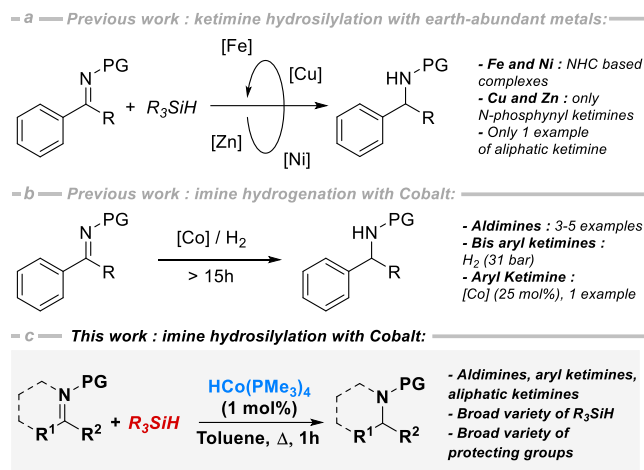
ABSTRACT. Herein we describe the formation and use of silyl cobalt(III) dihydride complexes as powerful catalysts for the hydrosilylation of a variety of imines starting from a low-valent well-defined cobalt(I) complex. The reaction is efficient at low catalyst loadings with a diverse range of imines bearing various protecting groups, as well as aliphatic ketimines and quinoline. Kinetics, DFT calculations, NMR spectroscopic studies, deuteration experiments and X-ray diffraction analysis allowed us to propose a catalytic cycle based on silyl dihydrocobalt(III) complexes performing a hydrocobaltation.

INTRODUCTION

Amines are key motifs in the living world given their essential role in amino acids in biology.¹ This function is omnipresent in agrochemicals, pharmaceuticals, and in bioactive or natural

molecules.² In this context, it is necessary to develop robust strategies to introduce amine groups onto molecules of interest. One of the most common strategies is the reduction of *N*-containing groups such as imine, nitrile, azide or nitro functions.³ Among these methods, the reduction of imines is advantageous as they are readily accessible from the corresponding ketones or aldehydes, providing facile access to structurally diverse and tunable substituted amines. Imines can be reduced by hydrogenation, hydrogen transfer or by reaction with hydrides.⁴ However, the direct hydrogenation of imines usually requires high hydrogen pressures. Given the innate and significant risks associated with the handling of pressurized hydrogen, these methods are often unfeasible, practically and economically, in an academic laboratory setting. While reactions with aluminum and boron hydrides such LiAlH_4 and NaXBH_3 ($X = \text{H}, \text{CN}\dots$) are operationally simple as they do not require additional metals, they face several drawbacks such as sensitivity to air, lack of functional group tolerance. Additionally, the stoichiometric requirement of hydrides leads to the generation of huge amounts of aluminum and boron waste. Recently, hydrogen transfer reactions have emerged as promising strategies to synthesize amine groups. Within this category of reactions, hydrosilylation is an appealing choice given the abundance of silicon on earth and the commercial availability of a variety of silanes which are fairly air stable and a lot easier to handle than hydrogen gas or metallic hydrides. Noble metals such as Ir, Ru, Rh, and Pd have been widely investigated for imine hydrosilylation.⁵ However, catalysis is currently facing the critical challenge of replacing these noble metals due to their low abundance, increasing cost and toxicity.⁶ Over the past few decades, impressive hydro-elementations strategies have been developed using main group catalysts (s-block and p-block) including strong Lewis acids, frustrated Lewis pairs (FLPs), commercially available bases and even catalyst-free conditions have been reported.⁷ In the field of catalyst-free hydro-elementation, hydrosilylation reactions are less studied than hydroboration.^{7e}

^{7g} Moreover, regarding the reduction of imines, aryl-imines are most commonly investigated with rare examples of alkyl ketimines.^{7c,8} Obviously, earth-abundant metals such as Fe, Ni, Cu, Zn and Co have also emerged as good alternative catalysts (Scheme 1a). Using these metals, very good results were obtained for the reduction of aldimines, and harsher conditions were generally necessary for the reduction of ketimines. In the specific case of Zn- and Cu-based catalysts, only ketimines bearing electron-withdrawing groups were reduced.⁹ Regarding Fe¹⁰ and Ni,¹¹ sophisticated ligands such as carbenes were required together with long reaction times and scarce examples of aliphatic ketimine reduction can be found in the literature. Cobalt is often described as the most mature non noble metal for cross-coupling reactions, C–H bond functionalization and more recently for the hydrogenation of unsaturated compounds.¹² However, its application towards the reduction of imines is still in its infancy.¹³ In fact, the direct hydrogenation of imines with cobalt under a H₂ atmosphere is limited to only four references in the literature (Scheme 1b). In 1986 Okamoto, a pioneer in this field, described the first example of imine hydrogenation using a bis(dioximato)cobalt quinine complex under mainly stoichiometric conditions.¹⁴ In 2012, Amézquita-Valencia and Cabrera described the use of Co₂(CO)₈/(*R*)-BINAP as the catalytic mixture for the asymmetric reduction of biphenyl ketimines.¹⁵ The same year Hanson described the use of a cobalt complex bearing a bis[2-(dicyclohexylphosphino)ethyl]amine ligand for the hydrogenation of various unsaturated bonds, including three aldimines but no ketimines were reduced.¹⁶ Finally, in 2014 Von Wangelin reported the use of an arene-cobalt complex for hydrogenations, but again, the scope of aldimines is narrow and no ketimine reduction was reported.¹⁷ Although some examples of hydrogenation are described, the use of silanes for the reduction of imines with cobalt complexes has not been reported in the literature.¹⁸

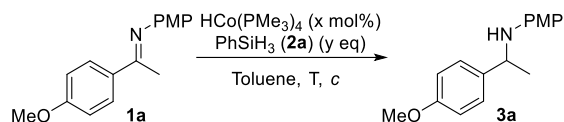


Scheme 1. Imine reduction with earth-abundant metals

During the last decade, our group¹⁹ and others²⁰ have been interested in the activity of two well-defined low valent cobalt complexes $\text{Co}(\text{PMe}_3)_4$ and $\text{HCo}(\text{PMe}_3)_4$ for bond activation. Using these two complexes, we have shown that simple catalysts can be competitive with noble metals for several applications. Moreover, using this “single-component catalyst” strategy,²¹ we were able to gain mechanistic insight into the hydroarylation and hydrosilylation of alkynes. From these previous studies, we determined that imines can easily enter cobalt’s coordination sphere and that various silanes can smoothly undergo oxidative addition onto these cobalt(0 or I) species.¹⁹

RESULTS AND DISCUSSION

With these observations in mind, we anticipated that these two low-valent cobalt complexes would be efficient catalysts for the hydrosilylation of imines (Scheme 1c). Table 1 summarizes our initial screening of reaction conditions.

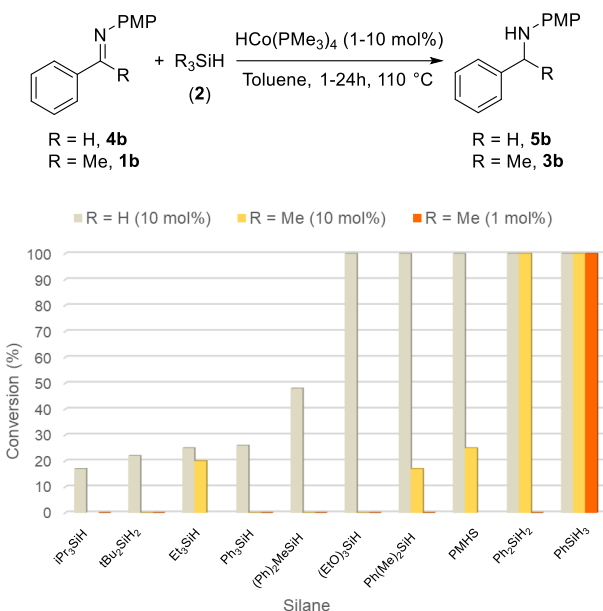
Table 1. Reaction condition optimization.^a

entry ^a	y (eq)	x (mol%)	T (°C)	Time	c	Conversion ^b
1	2	10	20	24h	0.25M	6%
2	2	10	50	24h	0.25M	53%
3	2	10	110	24h	0.25M	100%(73%) ^c
4	1	10	110	24h	0.25M	72%
5	2	5	110	24h	0.25M	100%
6	2	5	110	1h	0.25M	100%
7	2	2	110	1h	0.25M	50%
8	2	1	110	1h	0.25M	46%
9	2	1	110	8h	0.25M	58%
10	2	1	110	1h	1M	68%
11	2	1	110	1h	5M	100% (100%) ^d
12	2	– ^e	110	1h	5M	0%
13	–	1	110	24h	5M	0%

^aReaction conditions: **1a** (1 mmol, 1 eq), **(2a)** (y eq), HCo(PMe₃)₄ (x mol%, with respect to the imine), toluene (c); ^bConversion determined by ¹H NMR of the crude material; ^cNH₃BH₃ was used instead of PhSiH₃ ^dCo(PMe₃)₄ was used as the catalyst; ^eWith 4 mol% of PMe₃.

We chose ketimine **1a** as our model substrate and phenylsilane (**2a**) as the hydrogen donor. By using 2 equivalents of hydrogen donor and 10 mol% of HCo(PMe₃)₄ in toluene at room temperature, the reduction of the imine was observed but only in 6% conversion (Table 1, Entry 1). Reaction temperature has a significant impact on reaction efficiency, heating at 50 °C resulted in 53% conversion while a further increase to 110 °C allowed complete conversion (Table 1, Entries 1-3). Using NH₃BH₃ as a hydrogen donor instead of PhSiH₃ allows the formation of the desired amine, albeit with a lower yield of 73% (Table 1, Entry 3). Lowering the amount of silane

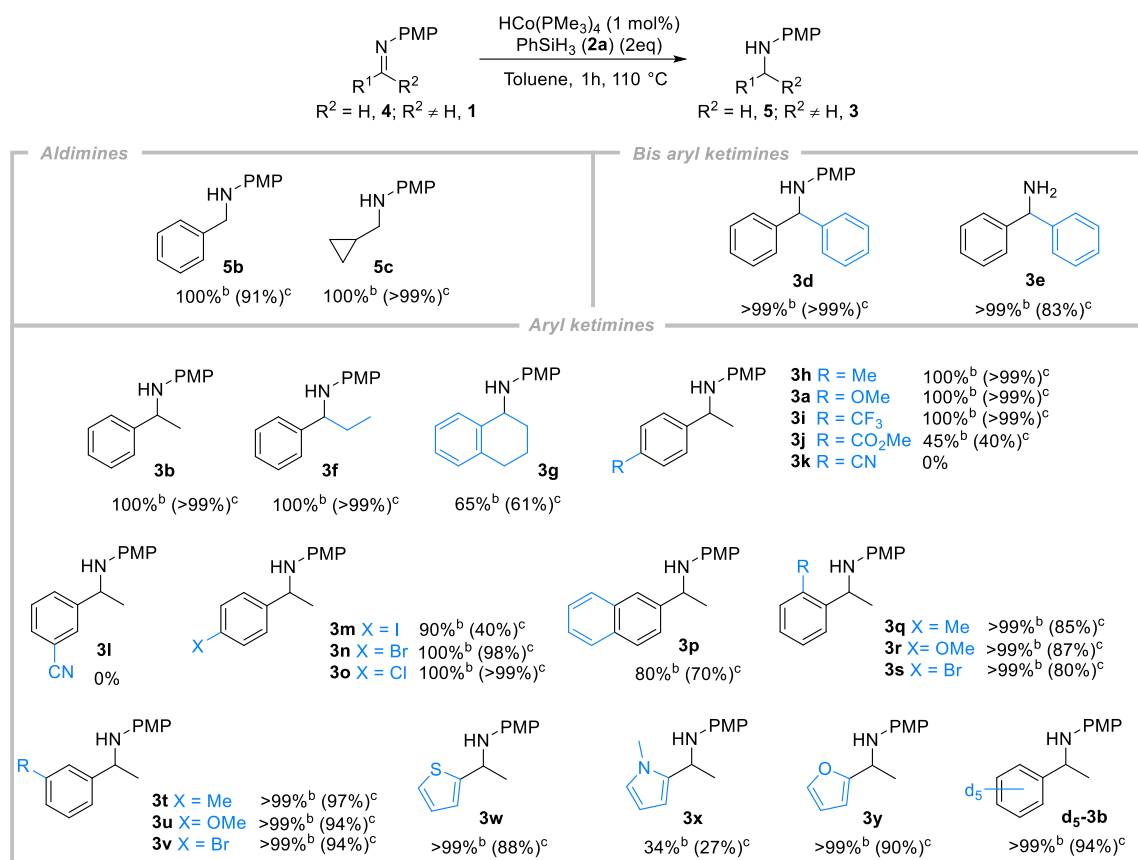
to 1 equivalent is detrimental as the conversion dropped to 72% (Table 1, Entry 4). On the other hand, the catalyst loading can be decreased from 10 to 5 mol% and the reaction time reduced to 1 hour without loss of conversion (Table 1, Entries 5 and 6). Attempts to further reduce the catalyst loading to 2 or 1 mol% results in decreased conversion even after 8 hours (Table 1, Entries 7-9). The key to reaching full conversion at 1 mol% of catalyst, was doubling the reaction concentration from 0.25M to 5M (Table 1, Entries 8, 10 and 11). Therefore, we defined Entry 11, Table 1, as our optimal reaction conditions. Notably, $\text{Co}(\text{PMe}_3)_4$ is equally effective as a catalyst for this transformation. However, to allow reaction monitoring via NMR spectroscopy and as it is easier to characterize, we selected the cobalt(I) hydride $\text{HCo}(\text{PMe}_3)_4$ as the sole catalyst for the entirety of the investigation. To prove that trimethylphosphine was not the catalyst of our reaction, we conducted a test experiment in presence of 4 mol% of trimethylphosphine instead of $\text{HCo}(\text{PMe}_3)_4$ that showed no conversion (Table 1, Entry 12).²² Moreover, no conversion occurred in the absence of silane, showing that it is the only source of hydrogen in our reaction medium (Table 1, Entry 13). Next, we screened the hydrogen donor efficiency of various silanes (**2**) in the reduction of phenylaldimine **4b** (Figure 1, beige bar, 10 mol% of catalyst) and phenylketimine **1b** (Figure 1, yellow bar 10 mol% of catalyst and orange bar 1 mol% of catalyst).



^aReaction conditions: **1b-4b** (1 mmol), **(2)** (2 mmol), HCo(PMe₃)₄ (1-10 mol%, with respect to the imine), toluene (0.2 mL), 110 °C, 24h (beige and yellow bars) or 1h (orange bar).

Figure 1. Screening of silanes **(2)** for the reduction of aldimine **4b** and ketimine **1b**^a

Almost all the silanes assayed can reduce aldimine **4b**, however alkyl and/or bulky ones are less efficient, with conversions below 50%. Moreover, almost all of them are inefficient for the reduction of ketimine **1b**. Five silanes led to full aldimine reduction, among them, triethoxysilane and PMHS appeared as cheap and stable alternatives for aldimines hydrosilylation. However, they were not reactive enough with ketimines even at 10 mol%. Diphenylsilane and phenylsilane both allowed full conversion of both aldimine **4b** and ketimine **1b** at this loading. However, only phenylsilane maintains its efficiency at lower catalyst loadings. With optimal conditions in hand, we sought to explore the potential scope of this hydrosilylation reaction. Various imines bearing a *p*-methoxyphenyl substituent as the protecting group were first selected for stability reasons.

Table 2. Hydrosilylation of aldimines **4** and arylketimines **1**^a

^a**1** or **4** (1 mmol), (**2a**) (2 mmol), HCo(PMe₃)₄ (1 mol%, with respect to the imine), toluene (0.2 mL), 110 °C, 1h; ^bConversion determined by ¹H NMR analysis of the crude material; ^cIsolated yield.

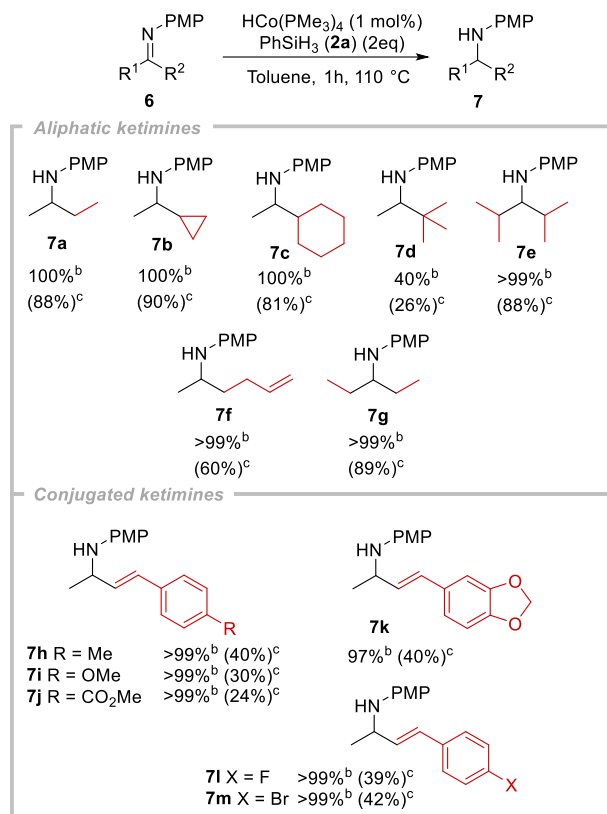
As aldimines **4** are less challenging substrates based on literature precedents, we chose to test only one aryl aldimine and one alkyl aldimine. As shown in the silane scope study, phenylaldimine **4b** was completely hydrosilylated and the corresponding amine **5b** can be isolated in 91% yield after work-up (Figure 1 and Table 2). Unsurprisingly, cyclopropylaldimine **4c** was easily reduced forming the corresponding amine **5c**, after work up, in quantitative yield. Bis-aryl ketimines such as **1d** and **1e** are also viable substrates affording amines **3d** and **3e** in quantitative and 83% yield, respectively. It is worth mentioning that the absence of a protecting group on imine **1e** has no

influence on its reactivity. By varying the substitution pattern at the alkyl moiety, we showed that imines derived from propiophenone **1f** and tetralone **1g** also yielded the desired amines in quantitative and 61% yield, respectively. The reaction proceeded in good yields for *para*-substituted aryl imines. Electron-donating (OMe, **1a**), neutral (Me, **1h**), and electron-withdrawing groups (e.g., CF₃, **1i**) were all tolerated and led to quantitative yields. Competitive experiments and DFT calculations were performed to detect any electronic effect depending on the substitution of the aromatic rings of the imines (see the Mechanistic Considerations part). Introduction of a methylester substituent at this position seems to have a deleterious effect on reactivity since only 45% conversion was obtained together with the recovery of the starting material **1j**. Introducing a nitrile onto the aromatic ring of the starting imine is completely detrimental to the reaction as **1k-1l** were fully recovered. Two hypotheses can be proposed: first, an electronic effect of the cyano substituent contributed to this unexpected lack of reactivity towards our catalyst; second, coordination of the Lewis basic nitrile substituent may poison the cobalt catalyst. To confirm the latter proposition, we ran a competitive experiment in acetonitrile (see Scheme S1) that demonstrated the inhibition of the catalyst in the presence of a nitrile moiety.

para-halogenated aryl imines **1m-o** also gave the desired amine in quantitative yield for chlorine and bromine substitution, and moderate yield for the iodine group that may be involved in oxidative addition side reactions. *ortho*- and *meta*-substituted imines **1q-v** with methyl, methoxy or bromine groups were well tolerated under reaction conditions and the corresponding amines **3q-v** were obtained in yields ranging from 80% to 97%. Heteroaryl rings such as thiophene, *N*-methylpyrrole, or furane in imines **1w-y** are compatible with our catalytic system and the amines **3w-y** are obtained in 88%, 27% and 90% yield, respectively. Finally, the deuterated analog of imine **1b** can be reduced in 94% yield. Importantly, the integrity of the perdeuterated aryl of the

amine was maintained, showing that, contrary to our previous study,^{19c} no C–H activation mechanism or intermediate is involved here.

Table 3. Hydrosilylation of aliphatic ketimines and α,β -unsaturated ketimines.^a

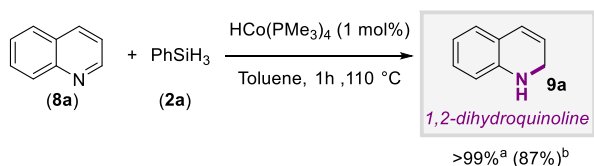


^a **6** (1 mmol), **(2a)** (2 mmol), HCo(PMe₃)₄ (1 mol%, with respect to the imine), toluene (0.2 mL), 110 °C, 1h; ^bConversion determined by ¹H NMR analysis of the crude material. ^cIsolated yield.

We then turned our attention towards the more challenging aliphatic ketimines and conjugated imines scarcely described in the literature (Table 3). To our delight aliphatic ketimines **6a-g** bearing ethyl, cyclopropyl, isopropyl, cyclohexyl, and homoallyl substituents proceeded efficiently under our optimal conditions and afforded the corresponding amines **7a-g** in good yields. Only compound **6d** bearing a *tert*-butyl group presented lower conversion most likely due to steric hindrance; the corresponding amine **7d** was obtained in 26% with recovery of the starting imine **6d**. On the contrary, ketimine **6e** substituted by two isopropyl groups does not suffer from

any loss of reactivity and the amine **7e** can be isolated in good yield (88%). Finally, imine **6f** bearing a terminal alkene on the alkyl chain provided the desired amine **7f** in 60% yield, showing no reduction of the alkene moiety. Thus, we proceeded with the hydrosilylation of α,β -unsaturated ketimines **6h-m**. All worked perfectly with full conversion and selectivity. However, given no concomitant reduction of the alkene, the desired allylic amines are prone to degradation and the isolated yields are low (24-42%).

Finally, we tested our catalytic system for the challenging reduction of aromatic heterocycle quinoline (**8a**) (Scheme 2).²³ Pleasingly, under the same reaction conditions, we observed complete conversion of quinoline and the formation of 1,2-dihydroquinoline **9a** in 87% yield. Notably, the selectivity of this reduction is excellent, as 1,2-dihydroquinoline **9a** was formed as a single regioisomer, with only traces of tetrahydroquinoline arising from over reduction.

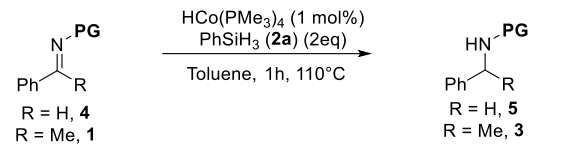


^aConversion determined by ¹H NMR analysis of the crude material; ^bIsolated yield

Scheme 2. Selective 1,2-reduction of quinoline (**8a**)

Our reaction scope (Tables 2 and 3) demonstrates the robustness of our procedure. Importantly, no change to catalyst loading or reaction time was necessary to reach almost full conversion for each substrate, which is often not the case in the literature. Finally, we investigated the compatibility of various imine protecting groups (see Table 4). We previously demonstrated that free imine **1e**, with no protecting group, could be efficiently hydrosilylated under these conditions (*vide supra* Table 2).

Table 4. Scope of the imine protecting group^a



Entry	R	PG	Conversion (%) ^b	Yield (%) ^c
1	H	PMP 5b	>99	91
2	H	Ph 5d	>99	92
3	H	Bn 5e	>99	82
4	H	SO ₂ Ph 5f	80	63
5	H	Ts 5g	60	47
6	H	^t Bu 5h	63	55
7	H	TMS 5i	>99	degradation
8	H	Boc 5j	>99	degradation
9	Me	<i>c</i> Pr 3ba	70	63
10	Me	Ph 3bb	>99	99
11	Me	<i>p</i> -CF ₃ Ph 3bc	>99	98

^a**1** or **4** (1 mmol), (**2a**) (2 mmol), HCo(PMe₃)₄ (1 mol%, with respect to imine), toluene (0.2 mL), 110 °C, 1h; ^bConversion determined by ¹H NMR analysis of the crude material; ^cIsolated yield.

Using commercially available aldimines (**4d-j**) we showed that aryl or benzyl protected aldimines (**4d**) and (**4e**) led to quantitative conversion and good isolated yields (92% and 82%, respectively) (Table 4, Entries 2 and 3). Arylsulfonyl protected imines such as (**4f**) and the tosyl (Ts) analog (**4g**) were less reactive and lower conversions and yields were observed (Table 4, Entries 4 and 5). In these cases we can postulate a potential ligation between the sulfonyl group and the catalyst that may slow down the reaction. Alkyl groups, such as *tert*-butyl, can be used (Table 4, Entry 6), albeit with a moderate 55% yield, probably due to the steric hindrance imposed. On the contrary, TMS- and Boc-protected aldimines (**4i**) and (**4j**) are not compatible with our reaction conditions and full degradation was observed (Table 4, Entries 7 and 8). Finally, ketimines **1ba**, **1bb** and **1bc** bearing

a cyclopropyl, a phenyl and a *para*-CF₃-phenyl protecting group, respectively, were all reactive and gave the desired amines **3ba**, **3bb** and **3bc** in 63%, 99% and 98% isolated yields, respectively (Table 4, Entries 9-11).

MECHANISTIC CONSIDERATIONS

In order to gain more mechanistic information, we monitored the evolution of the reaction *in situ* via ¹H NMR spectroscopy in a J. Young tube. For this experiment, we selected reaction conditions (Table 1, entry 5) with a concentration and a catalyst loading compatible with ¹H NMR spectroscopic analysis.

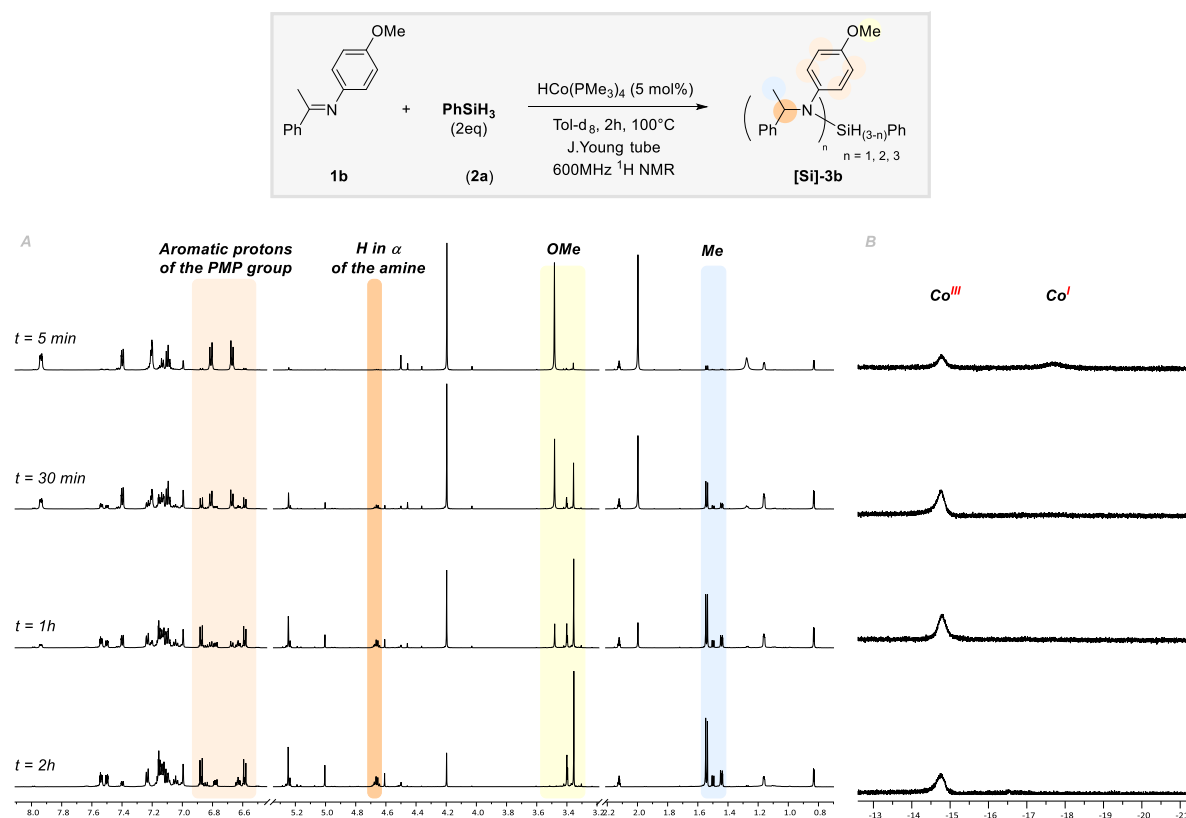
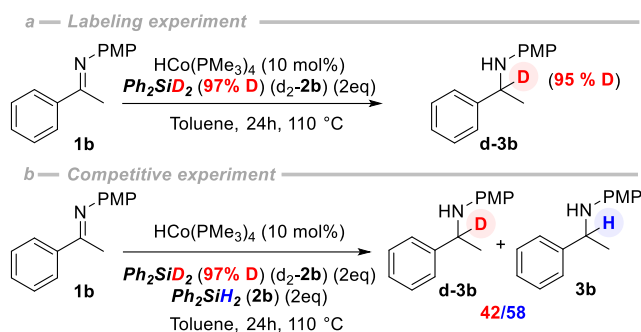


Figure 2. ¹H NMR spectrum (toluene-d₈, 600MHz, 373 K) evolution of the hydrosilylation reaction. A. ¹H area between δ 0.5 and 8 ppm, B. ¹H area between δ -21 and -13 ppm.

After 5 minutes, the hydride quintet at δ -17.31 ppm (Figure 2, area B), arising from the starting complex $\text{HCo}(\text{PMe}_3)_4$, has almost completely disappeared (see Supporting Information Figure S10 for more information) to form another complex with a hydride shifted at δ -14.76 ppm. Presumably, this new complex is obtained by oxidative addition of the $\text{HCo}(\text{PMe}_3)_4$ complex on PhSiH_3 (**2a**) to generate a new cobalt(III) specie (*vide infra* for studies dedicated to oxidative addition). The reaction is complete after 2 hours, as determined by observing the ^1H NMR spectrum. It is important to note that the products formed are silylated amines: this rules out a hydrogenation pathway and confirms the hydrosilylation process. Since we used PhSiH_3 (**2a**) we obtained a mixture of the aminosilane, the diaminosilane and some oligomers. However, after classical filtration on a pad of silica gel flushed with ethyl acetate, the free amine **3b** was obtained as the sole product (see Supporting Information Figure S11). Finally, the apparition of the quartet at δ 4.65 ppm, corresponding to the proton in the α position of the amine, shows that no incorporation of silane occurs at this position. It is worth mentioning that no hydride characteristic of a cobalt(I) complex was observed after 2 hours (Figure 2 area B). We also carried out deuteration experiments to rule out any enamine tautomers of ketimine.²⁴ Therefore, by using commercially available deuterated diphenylsilane (d_2 -**2b**) under our standard conditions, we observed the full incorporation of deuterium at the α position of the amine (Scheme 3a). This result confirms a direct hydrosilylation of the ketimines. Moreover, when using a 1/1 mixture of deuterated and non-deuterated silane, we obtained a 42/58 mixture of the deuterated amine **d-3b** and the non-deuterated one **3b** (Scheme 3b). The KIE of value 1.4 observed close to unity may suggest that the Si-H bond cleavage is not involved in the rate determining step of the reaction and that the formation of the C-H bond in the α position of the amine is a non-reversible step.²⁵



Scheme 3. a) Labeling experiment and b) Competitive experiment with Ph_2SiD_2 (**d₂-2b**)

As previously mentioned, we discovered during ^1H NMR spectroscopic monitoring, that a new cobalt complex rapidly formed in presence of the silane. We postulated the formation of cobalt(III) complex by oxidative addition of the silane as observed in our previous study on alkyne hydrosilylation.^{19e} To confirm our hypothesis we successfully isolated four silyl dihydride cobalt (III) complexes resulting from the oxidative addition of various silanes: PhSiH_3 (**2a**), Ph_2SiH_2 (**2b**),²⁶ Ph_3SiH (**2c**) and $(\text{EtO})_3\text{SiH}$ (**2d**) on $\text{HCo}(\text{PMe}_3)_4$ at 80 °C. The characterization of these species by ^1H NMR spectroscopy revealed a common tendency of the hydride peak to shift from δ -17.31 ppm for the $\text{HCo}(\text{PMe}_3)_4$ complex to δ -14.76, -14.66, -14.79 and -15.28 ppm, respectively (Figure 3). Moreover, the integration evolves from 1 H for the starting $\text{HCo}(\text{PMe}_3)_4$ cobalt complex **Co-I** to 2 H for the cobalt(III) adduct **CoSi**, together with the loss of one phosphine. These observations confirm the stoichiometric interaction between the silane and the cobalt(I) complex, probably via oxidation addition. Notably, heating these complexes overnight at 80 °C or 100 °C does not allow recovery of the starting $\text{HCo}(\text{PMe}_3)_4$ complex, suggesting non-reversibility of the oxidative addition step.

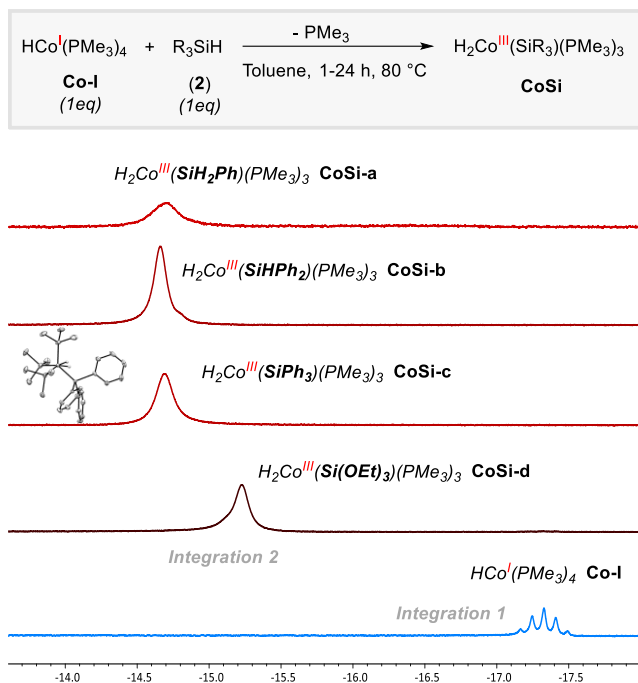


Figure 3. ^1H NMR spectrum (toluene- d_8 , 400 MHz) focused on the cobalt hydride area for the complexes **CoSi-a**, **CoSi-b**, **CoSi-c**, **CoSi-d** and **Co-I**

To our delight, we were able to obtain suitable crystals for X-ray diffraction analysis for triphenylsilyl dihydride cobalt (III) complex **2c** and confirmed the exact structure of these new cobalt(III) complexes **CoSi** (Figure 4).

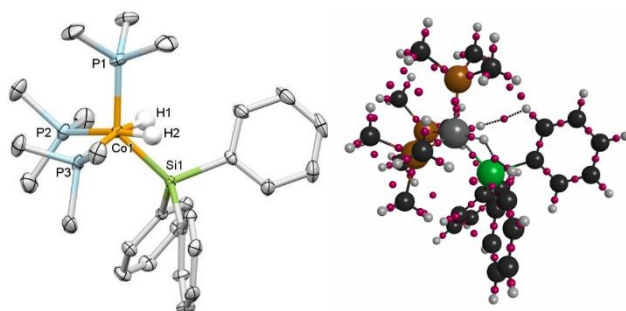


Figure 4. (Left) Solid-state molecular structure of $\text{CoH}_2(\text{SiPh}_3)(\text{PMe}_3)_3$ **CoSi-c**; Hydrogen atoms except the ones on Co and Si have been omitted for clarity. (Right) AIM analysis based on DFT calculations, purple balls indicate bond critical points.

At this point, The solid-state molecular structure of **CoSi-c** reveals an octahedron typical for a cobalt(III) complex, however the geometry is quite distorted. Complete oxidative addition seems to have occurred, as Si–H bond distances are longer than 2.00 Å. This is further confirmed by the short Co–H bond lengths of 1.40 and 1.33 Å. Compared to previously described dihydridosilylcobalt(III) complexes,²⁷ the distortion suggests an agostic interaction between the hydrogens and the silicon atoms. However, a NCIPLOT analysis based on DFT calculations reveals no strong dispersive interactions between the two hydrogens bonded to the cobalt and the silicon atoms. Interestingly, dispersion occurs between these hydrogen atoms and the phenyl groups of the silane (see Figure 4 right, dashed bonds). The Co–Si bond length of 2.24 Å is significantly longer than a possible silylene dihydride as shown recently by Tilley.²⁸

We were wondering if these silyl cobalt(III) dihydride complexes were the real active catalysts in the reaction. Using two isolated cobalt(III) dihydride complexes **CoSi-a** and **CoSi-d** we first ran stoichiometric experiments in a J. Young NMR tube with imine **1b** without addition of silane (Figure 5a1 and 5a2). We observed that the desired amine **3b** was obtained in 50% yield using the

complex synthesized from PhSiH_3 (**2a**). This suggests that **CoSi-a** could indeed be the catalyst of our reaction. Moreover, the same isolated complex **CoSi-a** used in a catalytic amount (1 mol%) in the presence of PhSiH_3 (**2a**) allowed full conversion to the desired amine, confirming this hypothesis (Figure 5b3 right). On the other hand, no amine was formed using the analog **CoSi-d** arising from $(\text{EtO})_3\text{SiH}$ (**2d**). This observation is in agreement with the catalytic approach as no ketimine reduction was observed in the presence of an excess of triethoxysilane as the reducing agent (Figure 1 and Figure 5b1-left). It is interesting to note that, starting from a catalytic amount of the isolated complex **CoSi-d**, however this time, in the presence of an excess of PhSiH_3 (**2a**), reactivity is restored and full conversion is achieved (Figure 5b2 right). Finally, we performed the reverse reaction (Figure 5b3). With a catalytic amount of **CoSi-a** in presence of an excess of $(\text{EtO})_3\text{SiH}$ (**2c**) no reaction was observed (Figure 5b3 left) but a post-addition of PhSiH_3 (**2a**) restored the reactivity and total conversion was observed (Figure 5b3 bottom). These last results suggest that PhSiH_3 (**2a**) is necessary for the reaction to turnover, probably through sigma-bond metathesis and not reductive elimination.²⁹ This is also confirmed by the fact that we never observed during the course of these reactions the (re)formation of any cobalt(I) species (see Figure 2 area B).

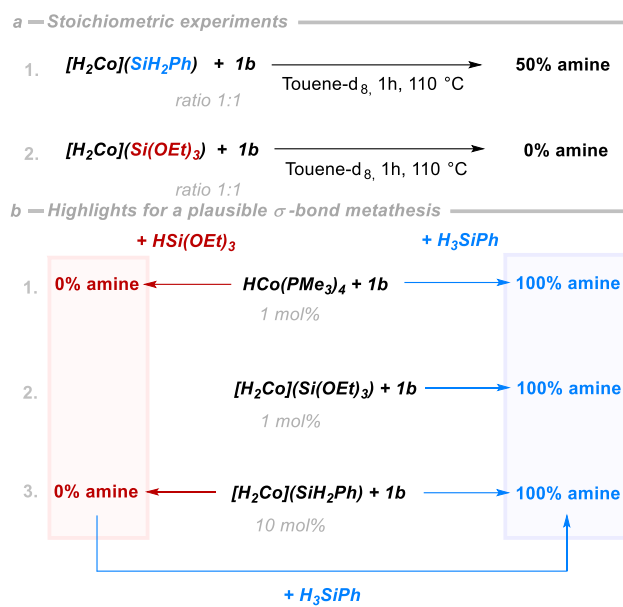


Figure 5. Reactivity of silyl cobalt(III) dihydride complexes **CoSi-a** and **CoSi-d** in presence of silanes (**2a**) and (**2d**). a) Stoichiometric experiments; b) Highlights for a plausible σ -bond metathesis

Kinetic studies were then conducted.²⁹ The oxidative addition step was studied by monitoring the disappearance of $HCo(PMe_3)_4$ **Co-I** over time by 1H NMR spectroscopy in the presence of an excess of phenylsilane (**2a**). The linear behavior of $\ln([Co^I]/[Co^I]_0)$ vs time and the linear plot of k_{app} vs $[Si]$ indicates that the first step of the catalytic cycle exhibits a first-order dependence on **Co-I** and on (**2a**) (see Figures S12 and S13). The catalytic hydrosilylation of imines was then studied by monitoring the consumption of the imine over time. The decay of **1b** over time was exponential (Figure 6a). All plots of $\ln[1b]$ vs time were linear indicating that the reaction has a first order dependence on **1b** (Figure 6b and Figures S14 and S15). We then varied the concentration of phenylsilane (**2b**) and catalyst **Co-I** independently. Linear plots of k_{obs} vs $[Si]$ (Figure 6c) and k_{obs} vs $[CoI]$ (Figure 6d) were obtained. We concluded that the reaction rate exhibits a first-order dependence on both (**2b**) and **Co-I**. To go further, kinetics studies were

conducted using **CoSi-a** as the catalyst. By varying its concentration, a linear plot of k_{obs} vs $[\text{Co}^{\text{III}}]$ (Figure 6e) was obtained, revealing that the reaction exhibits a first-order dependence whether starting from **Co-I** or from **CoSi-a**.

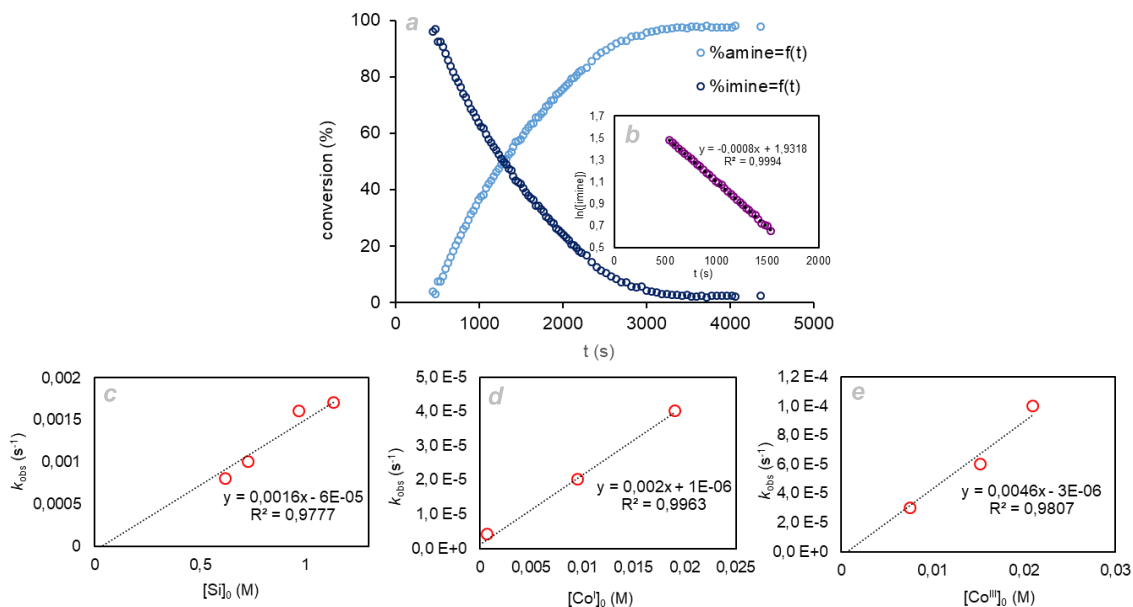


Figure 6 a) Reaction profile of the hydrosilylation of **1b** using phenylsilane (**2a**), **Co-I** as catalyst and 1,3,5-trimethoxybenzene as internal standard at 80 °C in toluene- d^8 . b) Plot of $\ln[\mathbf{1b}]$ vs time using the conditions of Figure 6a. c) Plot of k_{obs} vs $[\mathbf{2a}]_0$. All the k_{obs} were obtained from the slope of $\ln[\mathbf{1b}]$ vs time plots. d) Plot of k_{obs} vs $[\mathbf{Co-I}]_0$. All the k_{obs} were obtained from the slope of $\ln[\mathbf{1b}]$ vs time plots. e) Plot of k_{obs} vs $[\mathbf{CoSi-a}]_0$. All the k_{obs} were obtained from the slope of $\ln[\mathbf{1b}]$ vs time plots (see Figures S12 to S20).

Based on experimental observations, we can make some mechanistic assumptions.³⁰ One possibility could be that the reaction involves a radical mechanism. In fact, several radical additions onto imines have been described during the last two decades.³¹ Radical pathways, through hydrogen atom transfer (HAT), are normally proposed in the presence of an alkene and a metal hydride,³² the group of Chirik recently described that HAT mechanism can also occur using

a cobalt hydride complex under thermal conditions.³³ In our case, we ruled out a mechanism based on a radical pathway. Indeed, we chose aldimine **4c**, ketimines **1x** and **6b** bearing a cyclopropyl radical-clock substituent in some critical positions (on the nitrogen atom or in the alpha position). Whatever the substrate, we never observed the formation of compounds arising from the ring-opening of the cyclopropyl unit, typical of the formation of a radical in this position.³⁴ Moreover, when imine **6f** incorporating a pendent alkene moiety was evaluated in this reaction, no cyclization occurred either.

Additional mechanistic information was elucidated by performing DFT calculations using the Turbomole (version 6.5) suite of programs (Figure 7). The level of calculations was chosen to follow previous calculations conducted on $\text{HCo}(\text{PMe}_3)_4$: B3LYP as functional; complemented by the D3 dispersion scheme and using the def2-SV(P) basis set for describing orbitals.

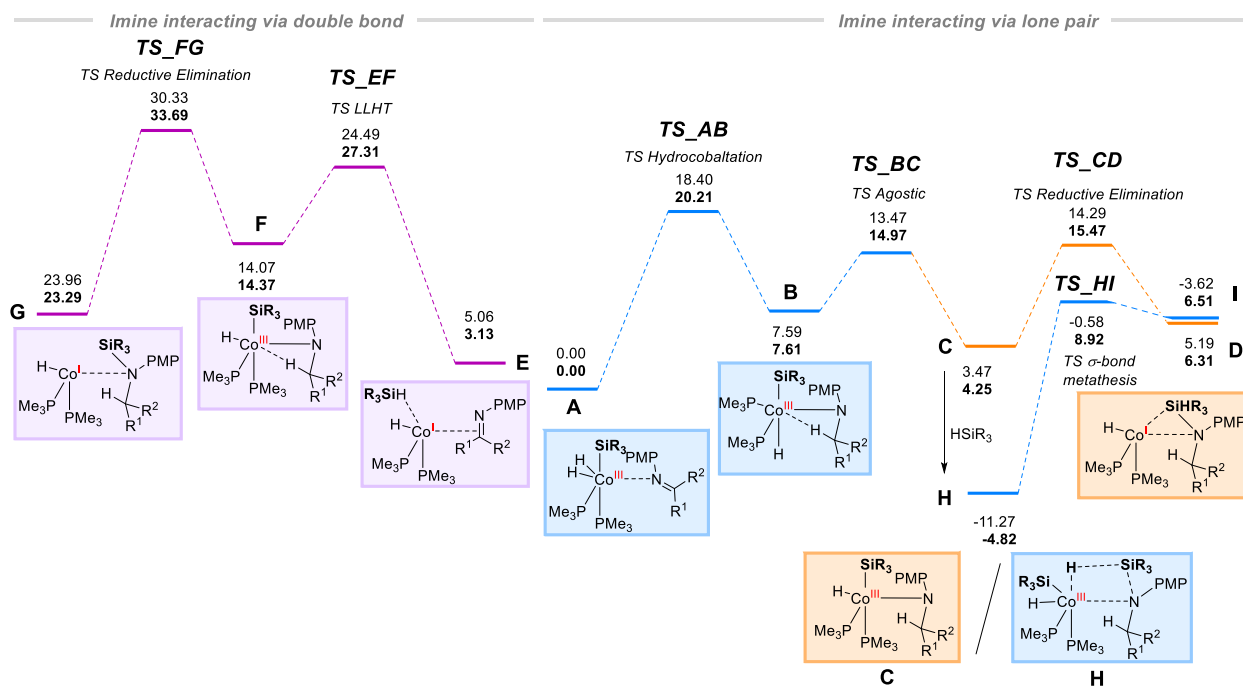


Figure 7. DFT calculated potential energy surfaces (in kcal.mol⁻¹) of the cobalt-catalyzed hydrosilylation of imines via the interaction with the double bond (on the left) and via the

interaction with the lone pair (on the right). Values in normal and bold fonts correspond respectively to the enthalpy and Gibbs free energies

Firstly, the cobalt complex $\text{HCo}(\text{PMe}_3)_4$ **Co-I** seems to be a pre-catalyst in the reaction. Due to the excess of silane (200 equivalents compared to the catalyst), a fast oxidative addition with the loss of one trimethylphosphine occurs to form the silylated cobalt(III) complex **CoSi**. A second trimethylphosphine is then exchanged with the imine, and at this stage, two different ligations of the cobalt to the imine can be envisioned: a ligation through the lone pair of the imine to give intermediate **A** or a π -ligation to generate **E** (Figure 7). Calculated structure **E** corresponds in fact to a complex in which the silane has not yet reacted with the cobalt center through oxidative addition. Thus it seems that the $\text{H}_2\text{Co}(\text{III})$ complex prefers coordination of the imine through the lone pair of the nitrogen. Three mechanistic possibilities can be now envisaged: a ligand to ligand hydrogen transfer (LLHT in purple) from the π -adduct intermediate **E**; or from the lone pair adduct **A**, a hydrocobaltation (in blue) or cobaltasilylation (not shown). The first mechanism that we can rule out based on calculations is cobaltasilylation: attempts to localize a transition state for this process gave barriers in the range of 50 kcal/mol. On the other hand, it is possible to localize a transition state from **A** corresponding to the hydrocobaltation process (**TS_AB**), with a barrier of 20.21 kcal/mol. The intermediate **B** obtained is characterized, in particular, by an agostic interaction between the transferred hydrogen and the cobalt center. To perform reductive elimination, it is necessary to first break this agostic interaction (**TS_BC**, barrier of 14.97 kcal/mol) to reach intermediate **C** which can undergo reductive elimination (in orange) with a barrier of 15.47 kcal/mol (**TS_CD**). It should be noted that the formation of product **D** is endothermic, however probably compensated by the numerous phosphines present in solution and not modelled here. Another possible termination of the catalytic cycle can also be a sigma-bond metathesis

between intermediate **B** and another silane molecule (in blue). Again, it is first necessary to break the agostic interaction to reach intermediate **H** and replace this interaction by the second silane. Since the postulated mechanism of sigma-bond metathesis involves a second silane, it was necessary to adjust our computational protocol to take into account the bimolecularity of the process. The remaining part of the computational exploration is unaffected by this modification. Namely, following the idea of Wertz³⁵ and Ziegler,³⁶ the gas-phase calculated entropies were divided by two in order to mimic the solvation process occurring during the course of the reaction. Hence, the approach of the second silane has a lower entropic cost reflecting its presence in large concentration. With this correction, we found that the metathesis mechanism has a barrier of 13.74 kcal/mol. Since the binding of the second silane is exothermic by 9.07 kcal/mol (from **C** to **H**), this process is much more favorable than direct reductive elimination that requires, in total, 20.29 kcal/mol from intermediate **H**. The other mechanistic possibility that we envisaged is to start from **E** and to perform imine reduction by avoiding oxidative addition on the metal. In that case, the mechanism would be reminiscent of the one we previously determined for C–H activation (*i.e.* Ligand to Ligand Hydrogen Transfer).^{19c} We found a barrier of 27.31 kcal/mol for this process (**TS_EF**), thus higher than the one for the process starting from **A**. The next step from intermediate **F** is the creation of the N–Si bond and the calculated energy is the highest one found during this mechanistic study (**TS_FG**, 33.69 kcal/mol). Therefore, it rules out the mechanism starting from imine interacting through π system, and reinforces the mechanism of hydrocobaltation followed by sigma-bond metathesis.

In order to obtain more insight on the electronic effect of the imine in the hydrocobaltation and the ligand exchange steps, we studied the variation of substituents on the *para* position of the two

phenyl groups by the DFT calculations (OMe, H and CF₃ as substituent) and no significant energy difference for the hydrocobaltation step was observed (Figure 8 right and left).

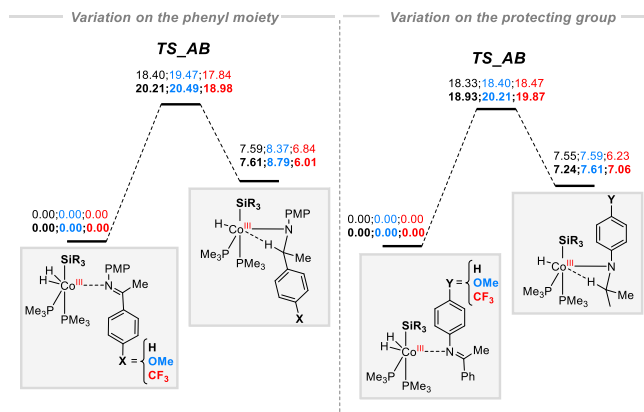


Figure 8. DFT hydrocobaltation step comparison by varying substituents on the imine moiety. Values in normal and bold fonts correspond respectively to the enthalpy and Gibbs free energies (in kcal.mol⁻¹).

We also ran two competition experiments at different temperatures (110 °C and 80 °C) with a deficit of silane and we followed the conversion by ¹H NMR spectroscopic analysis. While looking at the substitution of the aryl ring at the alpha position of the imine, no difference of reactivity was observed as these transformations led to a 1:1 mixture of both products (see Scheme S2), in accordance with our calculations. However, when looking at the nitrogen protecting group, the product ratio was 80/20 in favour of OMe substitution (see Scheme S3 and S4). The fact that the calculated hydrocobaltation energy was the same however with a difference in product ratio seems to indicate that ligand exchange could be the rate-limiting step of the catalytic cycle. To reinforce this hypothesis, we performed more DFT calculations. Notably, investigating the ligand exchange process with static DFT calculations is a complicated problem. Indeed, ligand exchange can either be an associative or a dissociative process, with implications of solvent molecules (first and second

layer of solvation). It is thus mainly a dynamic problem and obtaining realistic barriers requires extended ab-initio molecular dynamics simulations which was not studied here.

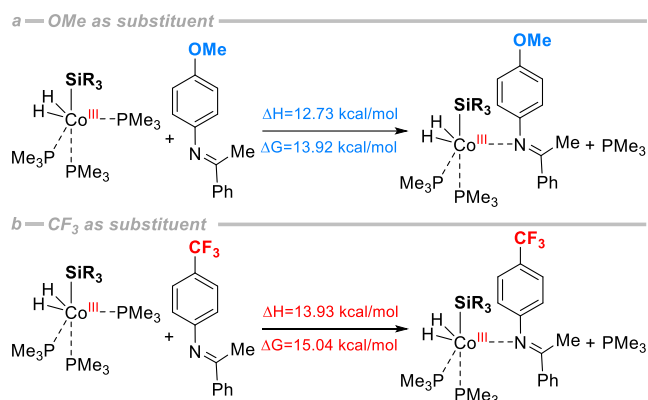
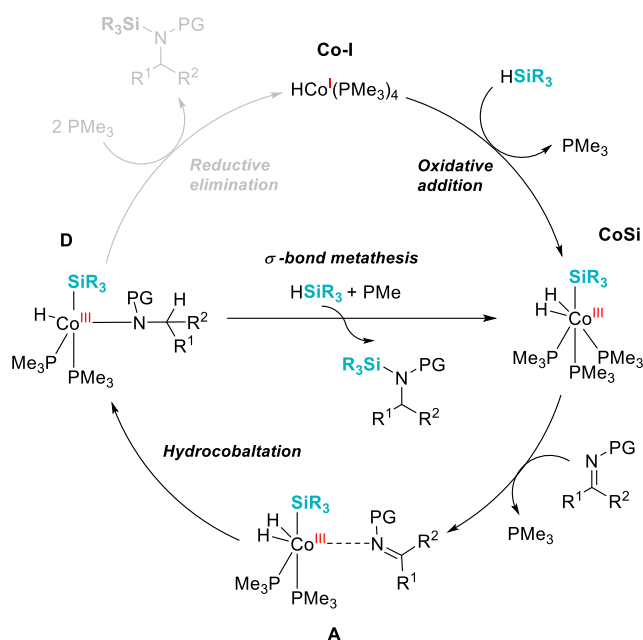


Figure 9. DFT calculations for phosphine exchange by imines.

On the other hand, we were able to calculate thermodynamic parameters for exchanging phosphine by various imines and we found this exchange is endothermic by around 15 kcal/mol (Figure 9). We note that the exchange by an imine bearing a CF₃ group is slightly more difficult than with a OMe group, which could explain the observed differences in reactivity (see Scheme S3). It also implies that barriers for this process are higher than 15 kcal/mol and thus probably higher than the hydrocobaltation step.

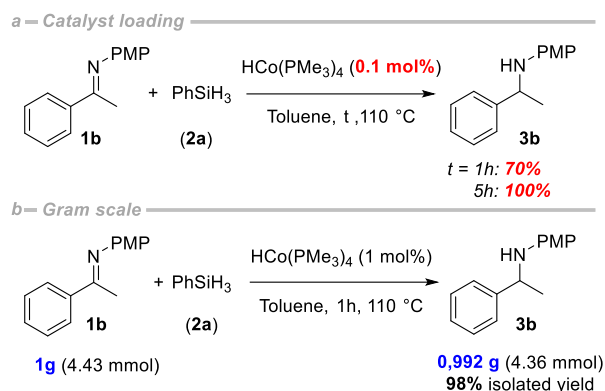


Scheme 4. Proposed mechanism for the hydrosilylation of imines

To summarize the proposed mechanism (Scheme 4), oxidative addition of the silane on the starting cobalt(I) complex **Co-I** generates the bis-hydrido cobalt(III) complex **CoSi**, with concomitant loss of one trimethylphosphine ligand. Then ligand exchange occurs between the imine and another phosphine, via a preferential interaction with the nitrogen lone pair. This exchange is probably the rate-limiting step of the catalytic cycle, based on DFT and kinetics studies. It forms intermediate **A** that undergoes hydrocobaltation on the imine to generate intermediate **D**. Sigma-bond metathesis³⁷ with the silane induces formation of the desired silylated amine and release of the cobalt(III) complex.

In order to test the limits of our reaction conditions we decided to decrease the catalyst loading to 0.1 mol% (Scheme 5a). Under these conditions, despite observation of a lower conversion (70%) after 1 hour, full conversion can be reached after 5 hours. Decreasing catalyst loading by a further factor of ten (0.01 mol%) led to only 5% of conversion and increasing reaction time to 24 hours

did not improve reaction outcomes. To prove the efficiency of our system we also ran a gram-scale experiment on imine **1b** that provided full conversion and an isolated yield of 98% (Scheme 5b).



Scheme 5. a) Catalyst loading limits and b) gram-scale reactions

CONCLUSION

In conclusion we have demonstrated the reactivity of well-defined or *in situ* generated silyl dihydride cobalt complexes obtained from the simple low-valent cobalt catalyst $\text{HCo}(\text{PMe}_3)_4$. Herein, we described the first hydrosilylation of imines catalyzed by a well-defined cobalt complex. This very robust hydrosilylation, with no change of conditions for all the substrates, is applicable on a large scope of imines including aldimines, aryl and aliphatic ketimines bearing various protecting groups but also on quinoline. The reaction conditions tolerate different functionalities and, for most of the imines, the reaction is over in less than one hour with a very low catalyst loading down to 0.1 mol%. Additionally, deuterium-labeling, kinetics, NMR spectroscopic and computational studies together with the X-ray characterization of a dihydrocobalt(III) intermediate have allowed us to propose a possible mechanism. The isolation, characterization and stability of such dihydrosilylcobalt(III) complexes is a huge step forward

regarding mechanistic disclosure. Their reactivity and modulation studies are currently under investigation in our laboratory.

ASSOCIATED CONTENT

The Supporting Information is available free of charge at <http://pubs.acs.org>.

Experimental procedures, DFT, kinetic studies and full spectroscopic data for all new compounds (PDF)

Crystallographic data for **CoSi-c** (CIF)

Crystallographic data for **1x** (CIF)

AUTHOR INFORMATION

Corresponding Author

*marc.petit@sorbonne-universite.fr

Funding Sources

This work was supported by CNRS, MRES and Sorbonne Université.

Notes

The authors declare no competing financial interest.

ACKNOWLEDGMENT

We warmly thank Geoffrey Gontard for X-ray structure of cobalt(III) complex **CoSi-d** and Dr. Brendan Fallon for fruitful discussions.

ABBREVIATIONS

AIM: Atoms in Molecules; BINAP: (2,2'-bis(diphenylphosphino)-1,1'-binaphthyl); Boc: *tert*-butoxycarbonyl; Bn: benzyl; Bu: butyl; *c*Pr: cyclopropyl; DFT: Density-functional theory; LLHT: ligand to ligand hydrogen transfer; NMR: nuclear magnetic resonance; PG: protecting group; Ph: phenyl; PMHS: Polymethylhydrosiloxane; PMP: *p*-methoxyphenyl; ppm: parts per million; TMS: trimethylsilyl; Ts: tosyl;

REFERENCES

¹ Molecular Biology of the Cell, 6th ed., Eds Alberts, B.; Johnson, A.; Lewis, J.; Morgan, D.; Raff, M.; Roberts, K.; Walter, P., New York: Garland Publishing, **2014**.

² a) Lawrence, S. A. Amines: Synthesis, Properties and Applications, Cambridge University Press, Cambridge, **2004**; (d) Ricci, A. in Amino Group Chemistry. From Synthesis to the Life Sciences, ed. A. Ricci, Wiley-VCH Verlag GmbH & Co. KGaA, Weinheim, **2008**.

³ a) Lévy, K.; Hegedűs, L. Recent Achievements in the Hydrogenation of Nitriles Catalyzed by Transition Metals *Curr. Org. Chem.* **2019**, *23*, 1881–1900; b) Formenti, D.; Ferretti, F.; Scharnagl, F. K.; Beller, M. Reduction of Nitro Compounds Using 3d-Non-Noble Metal Catalysts. *Chem. Rev.* **2019**, *119*, 2611–2680; c) Scriven, E. F. V.; Turnbull, K. Azides: their preparation and synthetic uses. *Chem. Rev.* **1988**, *88*, 297–368

⁴ Wang, D.; Astruc, D. The Golden Age of Transfer Hydrogenation. *Chem. Rev.* **2015**, *115*, 6621–6686.

⁵ Li, B.; Sortais, J.-B.; Darcel, C. Amine synthesis *via* transition metal homogeneous catalysed hydrosilylation. *RSC Adv.* **2016**, *6*, 57603–57625.

⁶ Chirik, P.; Morris, R. Getting Down to Earth: The Renaissance of Catalysis with Abundant Metals. *Acc. Chem. Res.* **2015**, *48*, 2495–2495.

⁷ a) Blackwell, J. M.; Sonmor, E. R.; Scoccitti, T.; Piers, W. E. B(C₆F₅)₃-Catalyzed Hydrosilylation of Imines via Silyliminium Intermediates, *Org. Lett.* **2000**, *2*, 24, 3921–3923; b) Manas, M. G.; Sharninghausen, L. S.; Balcells, D.; Crabtree, R. H. Experimental and computational studies of borohydride catalyzed hydrosilylation of a variety of C=O and C=N functionalities including esters amides and heteroarenes *New J. Chem.* **2014**, *38*, 1694–1700. c) Yin, Q.; Soltani, Y.; Melen, R. L.; Oestreich, M. BAr^F₃-Catalyzed Imine Hydroboration with Pinacolborane Not Requiring the Assistance of an Additional Lewis Base. *Organometallics* **2017**, *36*, 2381–2384; d) Elsen, H.; Fischer, C.; Knüpfer, C.; Escalona, A.; Harder, S. Early Main Group Metal Catalysts for Imine Hydrosilylation. *Chem. Eur. J.* **2019**, *25*, 16141–16147. e) Kuciński, K.; Hreczycho, G. Hydrosilylation and hydroboration in a sustainable manner: from Earth-abundant catalysts to catalyst-free solutions *Green Chem.*, **2020**, *22*, 5210–5224. f) Clarke, J. J.; Devaraj, K.; Bestvater, B. P.; Kojima, R.; Eisenberger, P.; DeJesus, J. F.; Crudden, C. M. Hydrosilylation and Mukaiyama aldol-type reaction of quinolines and hydrosilylation of imines catalyzed by a mesoionic carbene-stabilized borenium ion. *Org. Biomol. Chem.*, **2021**, *19*, 6786–6791. g) Pandey, V. K.; Donthireddy, S. N. R.; Rit, A. Catalyst-Free and Solvent-Free Facile Hydroboration of Imines. *Chem. - Asian J.* **2019**, *14*, 3255–3258.

⁸ Margeson, M. J.; Seeberger, F.; Kelly, J. A.; Leitl, J.; Coburger, P.; Szlosek, R.; Müller, C.; Wolf, R. Expedient Hydrofunctionalisation of Carbonyls and Imines Initiated by Phosphacyclohexadienyl Anions. *ChemCatChem* **2021**, *13*, 3761–3764.

⁹ a) Park, B-M.; Mun, S.; Yun, J. Zinc-Catalyzed Enantioselective Hydrosilylation of Imines. *Adv. Synth. Catal.* **2006**, *348*, 1029–1032. b) Park, B-M.; Feng, X.; Yun, J.-S. Enantioselective Hydrosilylation of Imines Catalyzed by Diamine-Zinc Complexes. *Bull. Korean Chem. Soc.* **2011**, *32*, 2960–2964. c) Lipshutz, B. H.; Shimizu, H. Copper(I)-Catalyzed Asymmetric Hydrosilylations of Imines at Ambient Temperatures. *Angew. Chem. Int. Ed.* **2004**, *43*, 2228–2230.

¹⁰ For selected examples and reviews with iron see: a) Shaikh, N. S. Sustainable Amine Synthesis: Iron Catalyzed Reactions of Hydrosilanes with Imines, Amides, Nitroarenes and Nitriles. *ChemistrySelect* **2019**, *4*, 6753–6777. b) Saini, A.; Smith, C. R.; Wekesa, F. S.; Helms, A. K.; Findlater, M. Conversion of aldimines to secondary amines using iron-catalysed hydrosilylation. *Org. Biomol. Chem.* **2018**, *16*, 9368–9372. c) Zhou, S.; Junge, K.; Addis, D.; Das, S.; Beller, M. A Convenient and General Iron-Catalyzed Reduction of Amides to Amines *Angew. Chem. Int. Ed.* **2009**, *48*, 9507–9510. d) Wei, D.; Darcel, C. Iron Catalysis in Reduction and Hydrometalation Reactions. *Chem. Rev.* **2019**, *119*, 2550–2610. f) Bhunia, M.; Hota, P. K.; Vijaykumar, G.; Adhikari, D.; Mandal, S. K. A Highly Efficient Base-Metal Catalyst: Chemoselective Reduction of Imines to Amines Using An Abnormal-NHC–Fe(0) Complex. *Organometallics* **2016**, *35*, 2930–2937. g) Misal Castro, L. C.; Sortais, J.-B.; Darcel, C. NHC-carbene cyclopentadienyl iron based catalyst for a general and efficient hydrosilylation of imines. *Chem. Commun.* **2012**, *48*, 151–153.

¹¹ Bheeter, L. P.; Henrion, M.; Chetcuti, M. J.; Darcel, C.; Ritleng, V.; Sortais, J.-B. Cyclopentadienyl N-heterocyclic carbene–nickel complexes as efficient pre-catalysts for the hydrosilylation of imines. *Catal. Sci. Technol.* **2013**, *3*, 3111–3116.

¹² Cobalt Catalysis in Organic Synthesis: Methods and Reactions; Hapke, M.; Hilt, G.; Eds, Wiley-VCH Verlag GmbH & Co. KGaA **2020**.

¹³ Ai, W.; Zhong, R.; Liu, X.; Liu, Q. Hydride Transfer Reactions Catalyzed by Cobalt Complexes. *Chem. Rev.* **2019**, *119*, 2876–2953.

¹⁴ Kobayashi, K.; Okamoto, T.; Oida, T.; Tanimoto, S. Cobalt-mediated Reduction of C=N Bond. Synthesis of Methyl *N-p*-Toluenesulfonyl-1-phenylglycinate Catalyzed by Bis(dioximato)cobalt–Quinine Complexes. *Chem. Lett.* **1986**, *15*, 2031–2034.

¹⁵ Amèzquita-Valencia, M.; Cabrera, A. The First Example of Asymmetric Hydrogenation of Imines with Co₂(CO)₈/(R)-BINAP as Catalytic Precursor. *J. Mol. Catal. A: Chem.* **2013**, *366*, 17–21.

¹⁶ Zhang, G.; Scott, B. L.; Hanson, S. K. Mild and Homogeneous Cobalt-Catalyzed Hydrogenation of C=C, C=O, and C=N Bonds. *Angew. Chem. Int. Ed.* **2012**, *51*, 12102-12106.

¹⁷ Gärtner, D.; Welther, A.; Rezaei Rad, B.; Wolf, R.; Von Wangelin, A. J. Heteroatom-Free Arene-Cobalt and Arene-Iron Catalysts for Hydrogenations. *Angew. Chem. Int. Ed.* **2014**, *53*, 3722–3726.

¹⁸ For a single example (with no yield) that is part of a high-throughput screening see: Ireland, T.; Fontanet, F.; Tchao, G.-G. Identification of new catalysts for the asymmetric reduction of imines into chiral amines with polymethylhydrosiloxane using high-throughput screening. *Tetrahedron Lett.* **2004**, *45*, 4383–4387.

¹⁹ a) Ventre, S.; Simon, C.; Rekhroukh, F.; Malacria, M.; Amatore, M.; Aubert, C.; Petit, M. Catalytic Version of Ene-ene Cobalt-Mediated Cycloaddition and Selective Access to Unusual Bicyclic Trienes. *Chem. Eur. J.* **2013**, *19*, 5830–5835. b) Ventre, S.; Derat, E.; Amatore, M.; Aubert, C.; Petit, M. Hydrido-Cobalt Catalyst as a Selective Tool for the Dimerisation of Arylacetylenes: Scope and Theoretical Studies. *Adv. Synth. Catal.* **2013**, *355*, 2584–2590. c) Fallon, B. J.; Derat, E.; Amatore, M.; Aubert, C.; Chemla, F.; Ferreira, F.; Perez-Luna, A.; Petit, M. C–H Activation/Functionalization Catalyzed by Simple, Well-Defined Low-Valent Cobalt Complexes. *J. Am. Chem. Soc.* **2015**, *137*, 2448–2451. d) Fallon, B. J.; Garsi, J.-B.; Derat, E.; Amatore, M.; Aubert, C.; Petit, M. Synthesis of 1,2-Dihydropyridines Catalyzed by Well-Defined Low-valent Cobalt Complexes: C-H Activation Made Simple. *ACS Catal.* **2015**, *5*, 7493–7497. e) Fallon, B. J.; Derat, E.; Amatore, M.; Aubert, C.; Chemla, F.; Ferreira, F.; Perez-Luna, A.; Petit, M. C2-Alkylation and Alkenylation of Indoles Catalyzed by a Low-Valent Cobalt Complex in the Absence of Reductant. *Org. Lett.* **2016**, *18*, 2292–2295. f) Rivera-Hernandez, A.; Fallon, B. J.; Ventre, S.; Simon, C.; Tremblay, M. H.; Gontard, G.; Derat, E.; Amatore, M.; Aubert, C.; Petit, M. Regio- and Stereoselective Hydrosilylation of Unsymmetrical Alkynes Catalyzed by a Well-Defined, Low-Valent Cobalt Catalyst. *Org. Lett.* **2016**, *18*, 4242–4245. g) Fallon, B. J.; Corcé, V.; Amatore, M.; Aubert, C.; Chemla, F.; Ferreira, F.; Perez-Luna, A.; Petit, M. A Well-defined Low-Valent Cobalt Catalyst $\text{RCo}(\text{PMe}_3)_4$ with Dimethylzinc: A Simple Catalytic Approach for the Reductive Dimerization of Benzyl Halides. *New J. Chem.* **2016**, *40*, 9912–9916. h) Ferrand, L.; Lyu, Y.; Rivera-Hernández, A.; Fallon, B. J.; Amatore, M.; Aubert, C.; Petit, M. Hydroboration and Diboration of Internal Alkynes Catalyzed by a Well-Defined Low-Valent Cobalt Catalyst, *Synthesis* **2017**, *49*, 3895–3904.

²⁰ For selected examples from other groups: a) Li, J.; Li, X.; Wang, L.; Hu, Q.; Sun, H. C–Cl bond activation and catalytic hydrodechlorination of hexachlorobenzene by cobalt and nickel complexes with sodium formate as a reducing agent. *Dalton Trans.* **2014**, *43*, 6660–6666. b) Beck, R.; Camadanli, S.; Flörke, U.; Klein, H.-F. Reaction cascade: Ortho-C–H activation and C–C coupling of benzophenone leading to tetranuclear organoiron and mononuclear organocobalt complexes. *J. Organomet. Chem.* **2015**, *778*, 47–55. c) Rajpurohit, J.; Kumar, P.; Shukla, P.; Shanmugam, M.; Shanmugam, M. Mechanistic Investigation of Well-Defined Cobalt Catalyzed Formal E-Selective Hydrophosphination of Alkynes. *Organometallics* **2018**, *37*, 2297–2304. d) Li, Y.; Krause, J. A.; Guan, H. Silane Activation with Cobalt on the POCOP Pincer Ligand Platform. *Organometallics* **2020**, *39*, 3721–3730.

²¹ Suslick, B. A.; Tilley, T. D. Mechanistic Interrogation of Alkyne Hydroarylations Catalyzed by Highly Reduced, Single-Component Cobalt Complexes. *J. Am. Chem. Soc.* **2020**, *142*, 11203–11218.

²² We investigated the possibility of an auto-catalyzed hydrosilylation by putting 10 mol% of deprotonated amine in absence of cobalt and no conversion was observed.

²³ Pang, M.; Chen, J.-Y.; Zhang, S.; Liao, R.-Z.; Tung, C.-H.; Wang, W. Controlled partial transfer hydrogenation of quinolines by cobalt-amido cooperative catalysis *Nat. Commun.* **2020**, *11*, 1249–1258.

²⁴ a) Hermeke, J.; Klare, H. F. T.; Oestreich, M. Direct Catalytic Access to N-Silylated Enamines from Enolizable Imines and Hydrosilanes by Base-Free Dehydrogenative Si–N Coupling. *Chem. Eur. J.* **2014**, *20*, 9250–9254. b) Pérez-Miqueo, J.; San Nacianceno, V.; Urquiola, F. B.; Freixa, Z.

Revisiting the iridacycle-catalyzed hydrosilylation of enolizable imines. *Catal. Sci. Technol.* **2018**, *8*, 6316–6329.

²⁵ A control experiment showed that a rapid scrambling between Ph₂SiH₂ and Ph₂SiD₂ is catalyzed by the HCo(PMe₃)₄ complex even at rt (See Supporting Information).

²⁶ This cobalt(III) complex with Ph₂SiH₂ was recently proposed as a key intermediate but not isolated see : Yang, Qi W.; Fan, Q.; Du, X.; Xie, S.; Huang, W.; Li, X.; Sun, H.; Fuhr, O.; Fenske, D. [P,C]-Chelate Cobalt(III) Hydride Catalyzed Hydrosilylation of Alkenes. *Organometallics* **2021**, *40*, 2836–2843.

²⁷ Mautz, J.; Heinze, K.; Wadepohl, H.; Huttner, G. Reductive Activation of tripod Metal Compounds: Identification of Intermediates and Preparative Application. *Eur. J. Inorg. Chem.* **2008**, 1413–1422.

²⁸ Handford, R. C.; Smith, P. W.; Tilley, D. T. Activations of all Bonds to Silicon (Si–H, Si–C) in a Silane with Extrusion of [CoSiCo] Silicide Cores. *J. Am. Chem. Soc.* **2019**, *141*, 8769–8772

²⁹ Nolin, K. A.; Krumper, J. R.; PLuth, M. D.; Bergman, R. G.; Toste, F. D. Analysis of an Unprecedented Mechanism for the Catalytic Hydrosilylation of Carbonyl Compounds. *J. Am. Chem. Soc.*, **2007**, *129*, 14684–14696.

³⁰ Lipke, M. C.; Liberman-Martin, A. L.; Tilley, T. D. Electrophilic Activation of Silicon–Hydrogen Bonds in Catalytic Hydrosilylations. *Angew. Chem. Int. Ed.* **2017**, *56*, 2260 – 2294.

³¹ a) Friestad, G. K. Addition of carbon-centered radicals to imines and related compounds. *Tetrahedron* **2001**, *57*, 5461–5496; b) Miyabe, H.; Yoshioka, E.; Kohtani, S. Progress in Intermolecular Carbon Radical Addition to Imine Derivatives *Current Organic Chemistry*, **2010**, *14*, 1254–1264; c) Garrido-Castro, A.F.; Maestro, M.C.; Alemán, J. α -Functionalization of Imines via Visible Light Photoredox Catalysis. *Catalysts* **2020**, *10*, 562–584.

³² Kyne, S. H.; Lefèvre, G.; Ollivier, C.; Petit, M.; Ramis Cladera, V-A.; Fensterbank, L. Iron and cobalt catalysis: new perspectives in synthetic radical chemistry. *Chem. Soc. Rev.*, **2020**, *49*, 8501–8542.

³³ Mendelsohn, L. N.; MacNeil, C. S.; Tian, L.; Park, Y.; Scholes, G. D.; Chirik, P. J. Visible-Light-Enhanced Cobalt-Catalyzed Hydrogenation: Switchable Catalysis Enabled by Divergence between Thermal and Photochemical Pathways *ACS Catal.* **2021**, *11*, 1351–1360

³⁴ Coeffard, V.; Thobie-Gautier, C.; Beaudet, I.; Le Grogneq, E.; Quintard, J-P. Mild Electrochemical Deprotection of N-Phenylsulfonyl N-Substituted Amines Derived from (R)-Phenylglycinol. *Eur. J. Org. Chem.* **2008**, 383–391.

³⁵ Wertz, D. H. Relationship between the gas-phase entropies of molecules and their entropies of solvation in water and 1-octanol. *J. Am. Chem. Soc.* **1980**, *102*, 5316–5322.

³⁶ Cooper, J.; Ziegler, T. A Density Functional Study of S_N2 Substitution at Square-Planar Platinum(II) Complexes. *Inorg. Chem.* **2002**, *41*, 6614–6622.

³⁷ We cannot totally exclude a mechanism through a reductive elimination.

